Nanostructured SiO$_x$ layers as substrates for liquid crystal local ordering. I. Functionalization to bind Bovine Serum Albumin

I. ZGURA, T. BEICA, S. FRUNZA[*], L. FRUNZA, P. GANEA, F. UNGUREANU, C. NEGRILA, A. NUTA[a],
A.-A. SORESCU[a], I. BUNEA[b], C. N. ZAHARIA[b]
National Institute of Materials Physics
[a]*National Institute for Research & Development in Chemistry and Petrochemistry*
[b]*Institute of Virology St. S. Nicolau of the Romanian Academy*

We present some results concerning deposition of silicon oxide layers SiOx-type onto glass plates. Such nanostructured layers of ca. 25 nm were deposited under vacuum at 60⁰ incidence angle. The layers were further functionalized to bind proteins. The layers were characterized by Fourier transform infrared spectroscopy and X-ray- photoelectron spectroscopy. We found that the silicon monoxide amount in the deposited samples is small and decrease more by a hydrophylization oxygen plasma treatment. Liquid crystal cells were then obtained to observe the molecular alignment imposed by such treated glass plates. The planar orientation of the liquid crystal molecules was observed in all the studied cases. A rather strong interaction of the organic layers with the substrate was then advanced leading to observed orientation.

1. Introduction

Self-assembled monolayers (SAMs) can be formed from alkanethiols on the surface of gold, either as single crystals or films [1-4]; these monolayers can further specifically bind proteins. If these bonds are produced in the presence of aligned liquid crystal (LC) molecules, the alignment is disturbed and thus reports the presence of the proteins [5-8].

In a previous work we have established the experimental conditions for the deposition of gold layers on the surface of glass plates by vaporization at small angle (large angle with the normal direction) forming nanostructured columnar semi-transparent layers [9a]. To improve the adherence of the gold layer on the glass without additional metallic depositions we have used arene containing films since their π-bonding interaction might be energetically favorable to stick the Au clusters [9b]. Thus we have used polystyrene layers deposited on the glass plates by spin coating from the polymeric solution. Further the gold layers were functionalized with hexadecanethiol and self assembled monolayers (SAMs) were formed [9c]. In all these cases, LC cells with the plates treated as mentioned were assembled and the orientation of the LC molecules was used to probe the uniformity of the organic surface. However, due to quick layer contamination, these procedures require mostly that all the operations be performed in specialized conditions which are less largely accessible. Therefore, we looked for LC alignment onto new nanostructured substrates which might also specifically bind proteins.

This work presents some results concerning the use of dielectric substrates of non-stoichiometric silica layers (SiO$_x$) [10,11]. These layers are nanostructured and were functionalized in the aim to bind proteins by further treatment firstly in oxygen plasma, then in solutions of 3-aminopropyl)triethoxysilan, disuccinimidyl suberate and finally of Bovine Serum Albumin (BSA). Test LC cells were obtained for each step of functionalization and the alignment of the pentyl cyanobiphenyl molecules was observed.

2. Experimental

Materials and processing

Glass plates of soda-lime microscope slide type of 75×25×1 mm (commercially available from Cole Parmer) were cut (37×25 or 25×8 mm) for deposition. Their cleaning was an essential step for further operations, having a crucial role especially for the adherence of the first layer and implicitly, for the good alignment of liquid crystals in the cells [10a]. The method consists in using a cleaning solution followed by its careful removing by ultrasonication (90°C), repeated rinses with current and then with deionized water. Optional rinsing with alcohol was also applied. The plates were dried at 120 °C.

SiOx deposition was performed from a (pure) silicon oxide coating material (Balzers) in vacuum using the installation B30.2 (Hochvakuum Dresden), at 60° angle from normal direction to the surface (small angle by surface), on clean glass plates. The deposition conditions

(deposition rate of 0.1 nm/s, vacuum of 1.3 mPa) were so set to obtain a layer with the thickness of about 25 nm (corresponding to a certain range measured at normal incidence by the method quoted in ref. [12]). In special cases, some platelets were deposited frontally with SiO$_x$ under the same conditions.

Plasma treatment in oxygen discharge at P = 0.4 mbar was performed for hydrophylisation of the SiO$_x$ deposited plates for 1h [13] in a Standard Plasma Systems, model PICO (Electronic Diener).

Silanization with (3-aminopropyl)triethoxy-silane (APES). After deposition of nanostructured layer, the glass plates were immersed for 3h at 80 °C in a solution of APES (10 wt%) in acetate buffer/acetic acid at pH = 5. The reacted plates were rinsed with deionized water and then dried at 120 °C for 3h [14].

Surface activation with disuccinimidyl suberate (DSS) consisted in further treatment of the APES treated plates by easy stirring 1h in a solution (1mM) of DSS in anhydrous methanol, solution obtained by diluting a solution of DSS in dimethylsulfoxide [14]. Rinsing was done with methanol and deionized water.

Coupling with albumin of the activated surface was performed using Bovine Serum Albumin from Pierce. A solution was prepared of 1mg BSA/1mL phosphate buffer (PBS), pH of 7.2 [14], contact time of 12h; rinsing was done with deionized water, and then the plates were slowly dried. An alternative of this coupling reaction was that using biotinylated Bovine Serum Albumin (Pierce) (BSA-b); all the reaction conditions were the same as in the case of BSA deposition.

After deposition of these layers, the corresponding plates were stored in a closed dry volume (drying box with silica gel) until measuring or using to obtain the liquid crystal cells.

The glass plates were noted below with symbols for each of the succesively deposited layers such as SiO60+P+APES+DSS+BSA meaning a glass plate containing the nanostructured layer of SiOx (60 being the incidence angle), a more hydrophylic layer resulted by plasma treatment (P), then an APES layer, a DSS one and a BSA one.

To characterize the deposited layers, X-ray photoelectron spectroscopy (XPS) and Fourier transform infrared spectroscopy (FTIR) were currently applied.

XPS studies used a spectrophotometer VG ESCA MkII with Al source (K$_\alpha$=1486.6 eV), at a take-off angle of 55° [15] and software SDP 32, S-PROBE. Peak positions were assigned by referencing the C1s peak to a binding energy of 285 eV and linearly shifting all other XPS peaks by an equal amount, as it is customary. Further processing to decompose the peaks used Gaussian curves.

Vibrational spectra were recorded between 4000 and 650 cm^{-1} with a Spotlight 400 FTIR imaging system (Perkin Elmer) in reflection scanning mode, each spectrum having a resolution of 4 cm^{-1}. The maximum nominal resolution was 6.25×6.25 µm per pixel. Because the typical sampling areas of interest were in a much higher range (namely of 8×25 mm), all settings were selected to improve acquisition speed and to reduce the size of the data sets. Therefore, only images of 500×500 µm of the plates were recorded with two scans per exposure.

Liquid crystals cells

Test asymmetric *LC cells* were further obtained from the deposited glass plates with layers on both plates. One of the plates (8×25 mm) was deposited with different layers as described above and another one (37×25 mm) (named reference plate or counter-plate) was treated with an alignment layer such as SiOx layer frontally deposited or at oblique incidence (60° from normal). In the case of SiOx frontally deposited, it was additionally unidirectionally rubbed leading to an orientation of the LC molecules contacting this plate, parallel to the rubbing direction. Assembling of such plates was performed as represented in Fig. 1a, namely the direction of the SiOx deposition in the sample plate SiO60 and of unidirectionally rubbing in the reference plate were at 90°. A twist texture is thus expected in which the LC molecules have a continuous variation between the two plates. In fact there might be two equivalent such twisted textures, see Fig. 1b.
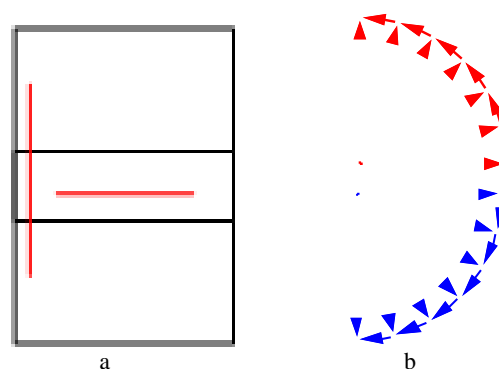

Fig. 1. a) Plates of deposited sample and of reference one assembled to impose a twist geometry in the cell. The lines corresponds to the alignment direction imposed by the sample plate (horizontal line) and by reference plate (vertical line). b) The two twisted textures compatible with the orienting directions upon the plates.

The cell thickness was 15 µm (established by Mylar spacer). For all cells, the plates were held together, especially during the handling of the cells, at two opposed ends using binder bulldog clips. The liquid crystal was 4*n*-pentyl-4'-cianobiphenyl (5CB) from Merck, having transition temperature nematic-to-isotrop of 35.4ºC. It was introduced in the cell mostly in the nematic state unless it was mentioned that 5CB was at 40ºC (in the isotropic state).

Optical examination of the LC cells was performed under crossed polarizers by direct visualization or in transmission mode on a polarized light microscope (Leitz Orthoplan) with a digital camera (Panasonic DMC-FZ8). Consistent settings of both the microscope light source

(numerical aperture 0.6) and the digital camera allowed for the direct comparison of images taken for different samples.

3. Results and discussion

The SiO_x deposition procedure leads to known structure of the layer. Thus, the SiO_x layer deposited at incidence of 60° (noted SiO_{60}) is columnary nanostructured while that deposited frontally (noted SiO) shows a rather flat surface. As opposite to other deposition procedures [16,17], the radial distribution of the evaporated species in our deposition chamber produces an enough narrow angular distribution [9a] in the columnar structure on the substrate. The structure of such SiO_{60} layer will be not further discussed. Instead, the layer properties revealed by IR spectroscopy and XPS are further presented. The IR spectra were studied considering the structural entities built around the Si–O–Si bridge by n oxygen atoms and $(6-n)$ silicon atoms that bond the bridge/edges. The interpretation of the Si(2p) XP spectrum is based on tetrahedral structures as Si(Si4), Si(Si_3O), Si(Si_2O_2), Si(SiO_3) and Si(O_4).

Local ordering inside the LC cells is then discussed in connection with the layer structure of the glass plates.

XPS investigations

Information about the presence of structural entities is obtained from XPS measurements.

Fig. 2 shows some representative spectra of the studied series. In the Si(2p) spectra, increasing the oxygen content by plasma treatment, an evolution towards higher binding energies of the main peak is observed. Such behavior has been reported before [18,19] and is explained by the charge transfer from Si to O atoms when Si-O bonds are formed.

Considering a tetrahedral configuration around silicon atom, the SiO_x structure is defined by several structural entities [20]. However, a fit of five corresponding Gaussian functions to the Si(2p) photospectra revealed that the main contributions to the material structure come from two structural entities. The results are exemplified in Fig. 3 for the sample SiO60: the main contribution belongs to Si(O_4) (peak A) and a very small contribution belongs to Si(Si_2O_2) structural entities (peak B).

a
b

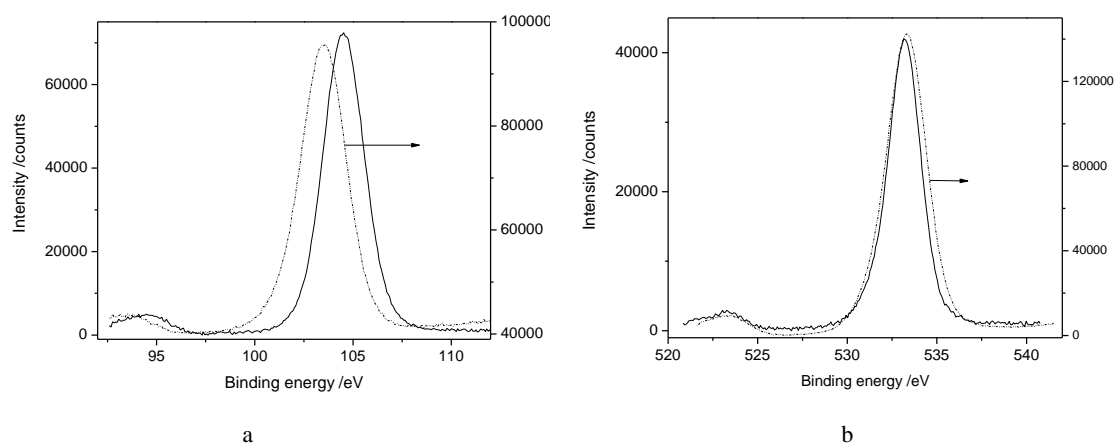*Fig. 2. High-resolution elemental XP spectra of the samples SiO60 (dotted line) and SiO60+P (continuous line). The spectra belong to a) Si(2p) and b) O(1s) core level.*

These findings concerning the peak position and full-width at half-maximum are in agreements with other works [21, 22] as well.

The O(1s) photoelectron spectrum contains three contributions. The dominant peak at a binding energy of 533.2 eV increasing by plasma treatment is characteristic to O^{2-} in SiO_2, the intermediate peak at 531.2 eV which decreases by plasma treatment is assigned to SiO_x species. The smallest peak is that at 535 eV.
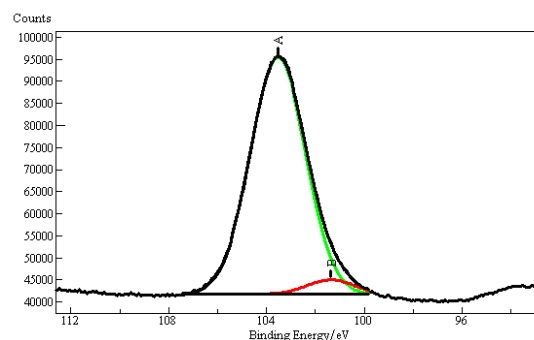

Fig. 3. The components and the best fit of the high-resolution Si(2p) photospectrum of the sample SiO_{60}.

FTIR investigations

The fingerprints of the Si-O-Si bonding group in an IR absorption spectrum are the vibrational rocking (350-500 cm^{-1}), bending (650-820 cm^{-1}) and stretching (940-1300 cm^{-1}) modes. In this paper, the attention is focused on the stretching mode, which is the strongest spectral feature seen in the experimental window. Fig. 4 shows the spectra in this region for all samples. Their analysis revealed a shoulder in the region 1100-1250 cm^{-1}, which is the fingerprint of the SiO$_2$ entity in the material structure. Its provenience is explained by Kirk [23] using a model of disorder-induced mechanical coupling between the active oxygen asymmetric stretch transverse-optic (TO) mode (in-phase motion of adjacent oxygen atoms) and the relatively optically inactive oxygen asymmetric stretch mode (out-of-phase motion of adjacent oxygen atoms). It was shown that a long-range coupling of these vibrational modes of Si-O-Si bridge produces a more flat shoulder. We conceive the shoulder shape as an indicator for the presence of SiO$_2$ amount in the layers. Thus, TO peak frequency is of 1062 cm^{-1} and LO peak frequency is of 1251 cm^{-1} [24]. The TO peak at 1080 cm^{-1} is characteristic of stoichiometric SiO$_2$.
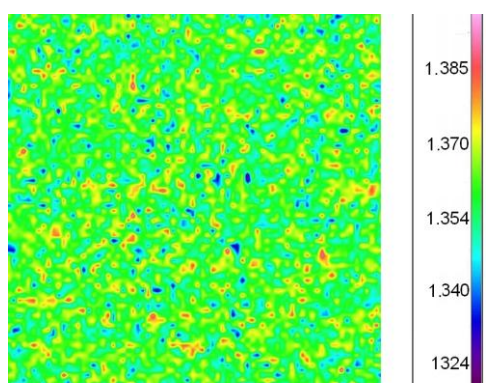

Fig. 3. FTIR image showing the distribution of SiO$_x$ layer in the sample SiO$_{60}$. Color scale on right indicates the integral value of the characteristic absorption band of the corresponding component.
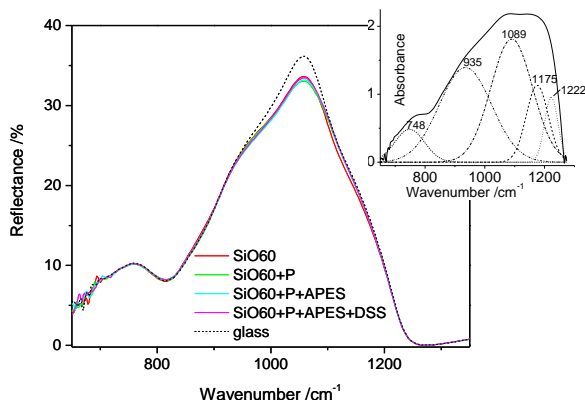

Fig. 4. Spectra in the range of Si-O bond vibrations extracted from FTIR images. The inset shows the decomposition of the peaks of glass sample into Gaussian components.

FTIR ''false-color composite'' images are formed on the basis of the inherent contrast that the unique chemical bonds of the various components in the sample. The variation in intensity is very small (1.316-1.400) and it is due to the non-uniform layer thickness. Fig. 3 then clearly shows the uniformity of the layer at the level of the considered pixel size.

All the spectra of the samples in Fig. 4 contain at least three peaks at ca. 1200, 1080, and 810 cm^{-1}, which are characteristic of bridging-oxygen vibrations. One observe that adding of each layer changes the reflection due to the main peak. An example of peak decomposition is given in the inset of Fig. 4.
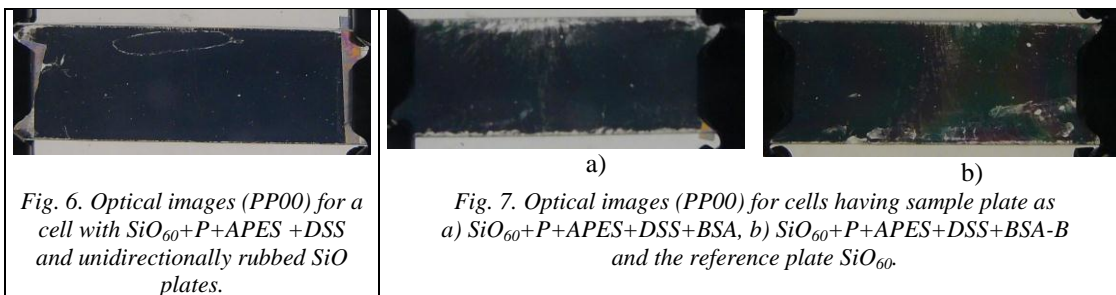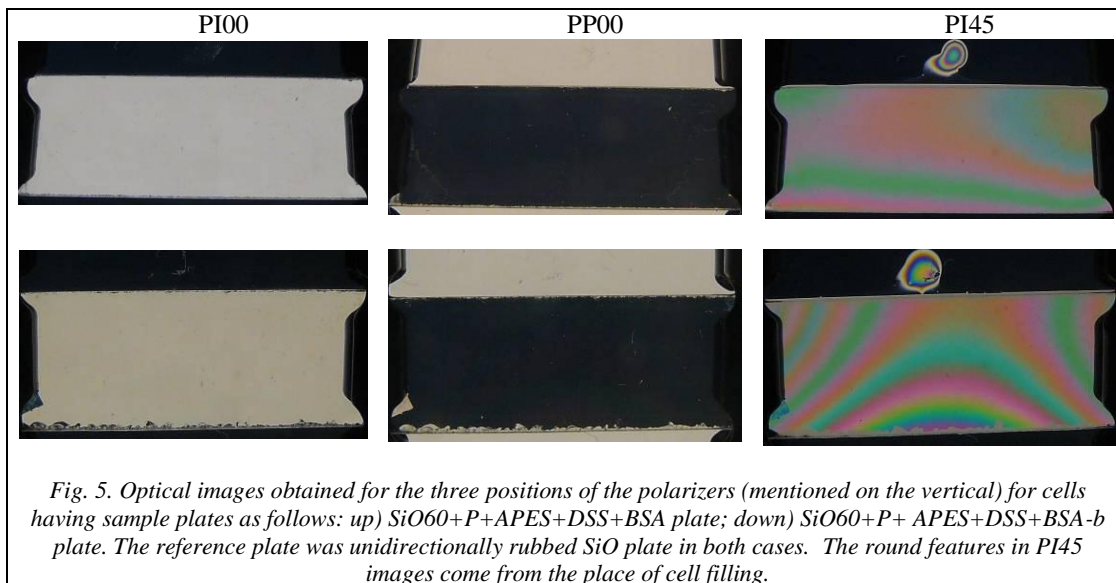
Liquid crystal cells

In the following are described the cells obtained from plates with successive deposited layers. The cells between polarizes appear as follows:
- Light between crossed polarizers (further called PI00 images).
- Dark between parallel polarizers (further called PP00 images.
- Colored between crossed polarizers but oriented at 45° from the preferred directions on the plates (further called PI45 images) most probably due to non-uniform thickness of the cell.

The reference plate imposes an orientation tangent parallel to the rubbing direction. The sample plates had incidence plane perpendicular to the long side so that the LC molecules orient tangent parallel to this side.

The influence of the reference plate can be followed by comparing the images in Fig. 5 with those in Fig. 7, in which the reference plate was deposited with nanostructured SiO$_x$ layer. In Fig. 7, the orientation corresponds to a typical twist cell, therefore it is not sensitive to the reference plate.

It is already known that the silicon oxide SiOx layer horizontally aligns liquid crystals when the value of x is in the range from about 1.0 to about 1.5, but vertically aligns the liquid crystals when the value of x is in a range from about 1.5 to about 2.0 [25]. In our cases, the composition of SiO$_x$ layer is very close to SiO$_2$ one. However, the orientation is different, maybe due to the more hydrophylic nature of the oxide, received by plasma treatment. The anchoring on SiO$_x$ has two origins [26]: long-range van der Waals potential and short-range surface interactions. Since the two origins have opposite preference in LC director orientation the observed transition is caused by the change of their relative strength. Thermal absorption-desorption of molecules on SiO$_x$ surface is important in determining the strength of short-range interactions, whereas the layer optical properties of SiO$_x$ are dependent on the van der Waals potential. The treatments applied to SiO$_x$ layer initiate transformations on the surface and provided new conditions at the interface. This leads to a change of slight axis orientation direction of LC molecules and appearance of various defects in the LC aligned structures [27]. It was suggested [28] that LCs are aligned by van der Waals interaction, more than by morphology effects.

PI00	PP00	PI45

Fig. 5. Optical images obtained for the three positions of the polarizers (mentioned on the vertical) for cells having sample plates as follows: up) SiO60+P+APES+DSS+BSA plate; down) SiO60+P+ APES+DSS+BSA-b plate. The reference plate was unidirectionally rubbed SiO plate in both cases. The round features in PI45 images come from the place of cell filling.

Fig. 6. Optical images (PP00) for a cell with SiO_{60}+P+APES +DSS and unidirectionally rubbed SiO plates.

Fig. 7. Optical images (PP00) for cells having sample plate as a) SiO_{60}+P+APES+DSS+BSA, b) SiO_{60}+P+APES+DSS+BSA-B and the reference plate SiO_{60}.

4. Conclusions

SiO$_x$ nanostructured layers were obtained by oblique evaporation onto glass plates. These layers preserve their ability to align nematic liquid crystals during successive treatments consisting in oxygen plasma discharge, silanization with solutions of 3-aminopropyl) triethoxysilane, functionalization with disuccinimidyl suberate and finally binding the Bovine Serum Albumins.

The planar alignment was observed in all the studied cases.

References

[1] R. G. Nuzzo, D. L. Allara, J. Amer. Chem. Soc. **105**, 4481 (1983).

[2] C. D. Bain, E. B. Troughton, Y.-T. Tao, J. Evall, G. M. Whitesides, R. G. Nuzzo, J. Amer. Chem. Soc. **111**, 321 (1989).

[3] M. D. Porter, T. B. Bright, D. L. Allara, C. E. D. Chidsey, J. Amer. Chem. Soc. **109**, 3559 (1987).

[4] G. M. Whitesides, P. E. Laibinis, Langmuir **6**, 86 (1990).

[5] V. K. Gupta, J. J. Skaife, T. B. Dubrovsky, N. L. Abbott, Science **279**, 2077 (1998).

[6] J. J. Skaife, J. M. Brake, N. L. Abbott, Langmuir **17**, 5448 (2001).

[7] Y.-Y. Luk, M. L. Tingey, D. J. Hall, B. A. Israel, C. J. Murphy, P. J. Bertics, N. L. Abbott, Langmuir **19**, 1671 (2003).

[8] L. A. Tercero Espinoza, K. R. Schumann, Y.-Y. Luk, B. A. Israel, N. L. Abbott, Langmuir **20**, 2375 (2004).

[9] a) T. Beica, S. Frunza, I. Zgura, L. Frunza, C. Cotarlan, C. Negrila, A.M. Vlaicu, C.N. Zaharia, J. Optoelectr. Adv. Mater. **12**, 347-353 (2010); b) I. Zgura, T. Beica, S. Frunza, O. Rasoga, A. Galca, L. Frunza, A. Moldovan, M. Dinescu, C. Zaharia, J. Optoelectr. Adv. Mater. **12**, 354 (2010); c) I. Zgura, T. Beica, S. Frunza, L. Frunza, C. Cotarlan-Simioniuc, F. Ungureanu, N. Gheorghe, O. Rasoga, T. Velula, C. Zaharia, J. Optoelectr. Adv. Mater. **12**, 1732 (2010).

[10] a) T. Beica, S. Frunza, M. Giurgea, R. Moldovan, Cryst. Res. Technol. **80**, 875 (1985); S. Frunza, R. Moldovan, T. Beica, M. Giurgea, D. Stoenescu,

Europhys. Lett. **20**, 407, (1992); b) S. Frunza, R. Moldovan, T. Beica, D. Stoenescu, M. Tintaru, Liq. Cryst. **14**, 293, (1993); c) S. Frunza, R. Moldovan, T. Beica, L. Georgescu, D. Stoenescu, M. Tintaru, Anal. Univ. Buc. Fiz. **42**, 57 (1993).

[11] a) R. Moldovan, G. Barbero, S. Frunza, T. Beica, Mol. Cryst. Liq. Cryst. **257**, 125 (1994); b) R. Moldovan, M.Tintaru, T. Beica, S. Frunza, D. N. Stoenescu, Rom. J. Phys. **42**, 353-358 (1997); c) R. Moldovan, S. Frunza, T. Beica, M. Tintaru, V. Ghiordanescu, Cryst. Res. Technol. **32**, 669-675 (1997).

[12] R. Moldovan, T. Beica, S. Frunza, M. Tintaru, Mol. Cryst. Liq. Cryst. **329**, 43 (1999).

[13] N. Preda, M. Enculescu, E. Matei, I. Enculescu, submitted 2010.

[14] S.-R. Kim, R. R. Shah, N. L. Abbott, Anal. Chem. **72**, 4646–4653 (2000).

[15] C. C. Negrila, C. Logofatu, R. V. Ghita, C. Cotirlan, F. Ungureanu, A. S. Manea, M. F. Lazarescu, J. Crystal Growth, 310, 1576 (2008).

[16] P. J. Martin, A. Bendavid, C. Comte, H. Miyata, Y. Asao, Y. Ishida, A. Sakai, Appl. Phys. Lett. **91**, 063516 (2007).

[17] K.-C. Kim, H.-J. Ahn, J.-B. Kim, B.-H. Hwang, H.-K. Baik, S. J. Lee, Jpn. J. Appl. Phys. **44**, 8071 (2005).

[18] F. J. Himpsel, F. R. McFeely, A. Taleb-Ibrahimi, J. A. Yarmoff, G. Hollinger, Phys. Rev. **B38**, 6084 (1988).

[19] R. Alfonsetti, L. Lozzi, M. Passacantando, P. Picozzi, S. Santucci, Appl. Surf. Sci. **70/71**, 222 (1993).

[20] N. Tomozeiu, J. J. van Hapert, E. E. van Faassen, W. Arnoldbik, A. M. Vredenberg, F. H. P. M. Habraken, J. Optoelectron. Adv. Mater. **4**, 513 (2002).

[21] L. M. Eshelman, A. M. de Jong, J.W. Niemantsverdriet, Catal. Lett. **10**, 201 (1991).

[22] F. Rebib, E .Tomasella, E. Bêche, J. Cellier, M. Jacquet, J. Phys.: Conf. Ser. **100**, 082034 (2008).

[23] C. T. Kirk, Phys. Rev. B **38**, 1255 (1988).

[24] K. T. Queeney, N. Herbots, Justin M. Shaw, V. Atluri, Y. J. Chabal, Appl. Phys. Lett. **84**, 493 (2004)

[25] S.-J. Rho, B.-K. Jeon, K.-O. Park, H.-K. Lee, H.-K. Baik, K.-C. Kim, J.-B. Kim, B.-H. Hwang, D.-C. Hyun, H.-J. Ahn, US Pattent 0279562 (2007).

[26] C. Chen, P. J. Bos, J. E. Anderson, Liq. Cryst., **35**, 465 (2008).

[27] Yu. Kolomzarov, P. Oleksenko, V. Sorokin, P. Tytarenko, R. Zelinskyy, Semicond. Phys., Quant. Electron. & Optoelectron. **9**, 60 (2006).

[28] K.-C. Kim, H.-J. Ahn, J.-B. Kim, B.-H. Hwang, H.-K. Baik, Langmuir **21**, 11079 (2005).

_____

[*]Corresponding author: lfrunza@infim.ro

.